

Preparation of zeolite N from metakaolinite by hydrothermal method

Paiboon Sengyang^a, Kunwadee Rangriwatananon^b and Apheruk Chaisena^{a,*}

^aDepartment of Chemistry and Center of Excellence for Innovation in Chemistry, Faculty of Science, Lampang Rajabhat University, Lampang 52100, Thailand

^bSchool of Chemistry, Institute of Science, Suranaree University of Technology, Nakhon Rachasima 30000, Thailand

Zeolite N was successfully prepared from activated Narathiwat kaolinite. Kaolinite activation was performed by the thermal treatment at 700 °C for 5 h. The thermally activated, amorphous kaolinite (metakaolinite) was treated hydrothermally with KOH, KCl, and H₂O at 80, 90, 110, 130, 150, and 175 °C during different reaction times ranging from 2 h to 24 h. The synthesis products were characterized by X-ray diffraction, scanning electron microscopy, Fourier transform infrared spectroscopy in order to elucidate their physicochemical and characteristics. The results show that zeolite N was obtained with high crystalline when the K₂O/Al₂O₃, KCl/Al₂O₃, and H₂O/Al₂O₃ molar ratios were 2.3, 3.5, and 48.0 by hydrothermal treatment at 175 °C for 24 h. The cation exchange capacity of zeolite N was 590 meq 100 g⁻¹. Thus, the kaolinite can be used as a source of silica and alumina for the synthesis of zeolite N.

Key words: zeolite N, Hydrothermal method, Metakaolinite, Alkaline treatment, Thermally activated kaolinite.

Introduction

Zeolite N or zeolite K-F(Cl) is a potassium-rich aluminosilicate of a general formula, K₁₂Al₁₀Si₁₀O₄₀Cl₂·8H₂O, for which a crystal structure has been determined by Christensen and Fjellvag [1]. Synthesis of zeolite N is under static hydrothermal conditions at 300 °C for a period of 7 days using zeolite 4A and excess potassium chloride. One remarkable discovery from the work of Mackinnon *et al.* [2] was the revelation of the possibility of synthesizing zeolite N at very mild temperature (<100 °C). Their work presented a new data on the synthesis of zeolite N at low temperature for a range of starting composition in a continuously stirred reaction. The reaction used kaolinite and montmorillonite as the source of silicon and aluminum. These conditions required a lower temperature and a shorter time than the one previously reported by Christensen and Fjellvag [1]. Zeolite N has been identified as a viable material for selection ion exchange application, particularly for the exchange of ammonium ion in aqueous solution [2]. The synthesis of zeolite can be carried out from clay minerals. Previous work has shown that the improvement of the properties of the kaolinite through chemical methods is difficult due to its low reactivity. This is because it was not significantly affected by acid or alkaline treatments, even with strong conditions [3-9]. Therefore, kaolinite is usually used after calcinations at temperatures between 550-950 °C [10] to obtain a more reactive phase

(metakaolinite), with the loss of structural water and associated reorganization of the structure. A small part of AlO₆ octahedra is maintained, while the rest is transformed into much more reactive tetra- and penta coordinated units [11-14]. Because of its availability and low cost, most industrial production processes presently utilize kaolinite and metakaolinite in the manufacture of zeolite. However, no previous attempt has been made to produce zeolite N from Narathiwat kaolinite. As a result, this work aimed at looking at the suitability of metakaolinite to synthesize the zeolite N and therefore to characterize it.

Experimental Procedure

Raw materials

Kaolinite was obtained from Narathiwat Province (Thai Clay Mineral Ltd.), Thailand. The Kaolinite samples were ground in agate mortar and sieved with a mesh number 63 micron aperture sieved while the metakaolinite was prepared by heating the kaolinite at 700 °C for 5 h in muffle furnace. The metakaolinite was characterized by X-ray diffraction (XRD) technique, Fourier transform Infrared (FTIR) spectroscopy, X-ray fluorescence (XRF) analysis. The reagents used to activate the metakaolinite were potassium hydroxide, as pellets (85%, from Volchem), potassium chloride, as pellets (99.8% from Volchem), and distilled water through standard purification methods.

Hydrothermal synthesis

The synthesis conditions for transformation of the metakaolinite using KOH and KCl as activating agents

*Corresponding author:
Tel : +66-054-241052
Fax: +66-054-241052
E-mail: apheruk@lpru.ac.th

were adapted from previous studies done by Mackinnon *et al.* [15-16]. Synthesis procedures involved the dissolution of KOH and KCl in water, stirring and heating the reaction to 95 °C, while the solution was carried out at the same temperature. Then the required amount of metakaolinite was added. Next, pH of the reaction gels was measured. Generally, the pH of this reaction mix is greater than 14.0 but the reaction was approximately reduced to 13.5 during the course. During the reaction process about 1.5 h to 3.5 h after the metakaolinite was added to the reactor, the viscosity of the mixture to increase small amounts of water was added up to aid mixing of the slurry although this adding was not necessary to achieve production zeolite N. The mixing reaction at temperature 95 °C ± 5 °C was carried out by hydrothermal synthesis under static conditions in PTFE (polytetrafluoroethylene = Teflon) digestion bomb (No. 4748, Parr.Inst.). The hydrothermal experiment was performed in an oven at 80, 90, 110, 130, 150, and 175 °C with controller (± 1 °C) with different reaction times (2, 6, 10, 12, and 24 h). After the hydrothermal treatment, the reaction mixtures were filtered, washed with distilled water. Then the products dried in an oven at 80 °C were kept in plastic bags for characterization.

Characterization techniques

Powder X-ray diffraction data were collected on a Bruker D5005 type diffractometer operating in Bragg-Brentano geometry. The radiation applied was Cu-K_α radiation (35 kV and 35 mA) and secondary monochromation. The samples were measured in step scan mode with steps of 0.3 degree / 0.02 second. Phase identification was made by searching the ICDD powder diffraction file database, with the help of Joint Committee on Powder Diffraction Standards (JCPDS) files for inorganic compounds. A JSM-5410V scanning electron microscopy (SEM) with INCA software by Oxford for energy dispersive X-ray spectroscopy (EDS) was utilized to estimate the element composition of different regions of the product. For SEM and EDS samples preparation, samples were placed on a brass stub sample using carbon tape. Then, the samples were dried with infrared light. After that, the samples were coated with a layer of gold approximately 20-25 Å thick using a Balzer sputtering coater to make them conductive. The micrographs were recorded with an acceleration voltage of 15 kV and at 3500-5000x magnification. FTIR was employed to study structure features. FTIR spectra were gained through a Shimadzu 8900 FTIR spectrometer in 400 to 1400 cm⁻¹ region by the KBr pellet technique. The spectra were obtained using an average of 45 scans with 8 cm⁻¹ resolution. Cation exchange capacity (CEC) values were verified through the ammonium acetate method [17]. This property was determined by equilibrium exchange of ammonium ions in a 1M ammonium acetate solution.

Samples were analyzed for ammonium ion concentration through the steam distillation method by Kjeldahl with bromocresol green indicator. The results were expressed as milliequivalents per 100 g of solids.

Results and Discussion

Characterization of kaolinite and metakaolinite

The chemical analysis of both the kaolinite and calcined kaolinite (metakaolinite) are presented in Table 1. The result shows the major element composition of the kaolinite as follows: SiO₂ (49.18), Al₂O₃ (37.61), and Fe₂O₃ (0.38) wt%. Chemical composition of kaolinite sample after calcination is SiO₂ (52.62), Al₂O₃ (40.94), and Fe₂O₃ (0.45) wt%, respectively. The amount of SiO₂ and Al₂O₃ presented in the kaolinite and metakaolinite indicated a ratio of SiO₂:Al₂O₃ as 1:30 and 1:28, which is greater than 1. This is in accordance with Breck [18] specification of clays for zeolite synthesis. The kaolinite, with its chemical stability, must be transformed into metakaolinite by the calcinations treatment at 700 °C. Dehydroxylation by a heat treatment converts the kaolinite into metakaolinite, which is an amorphous phase [19]. Amorphous phase is more reactive and easily reacted by alkalis. Fig. 1 shows the diffractogram of kaolinite sample consists of kaolinite (K), quartz (Q), and illite (I). However, metakaolinite being calcined at

Table 1. Chemical composition of kaolinite and metakaolinite.

Chemical analysis (wt % oxide)	Kaolinite	Metakaolinite
SiO ₂	49.18	52.62
Al ₂ O ₃	37.61	40.94
Fe ₂ O ₃	0.38	0.45
CaO	0.02	0.03
K ₂ O	1.13	1.25
TiO ₂	0.87	0.93
MgO	0.24	0.24
Na ₂ O	0.13	0.01
LOI	0.87	0.92

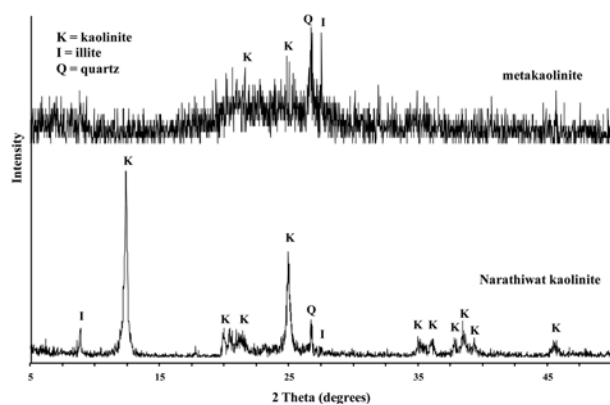


Fig. 1. X-ray diffraction pattern of Narathiwat kaolinite and metakaolinite.

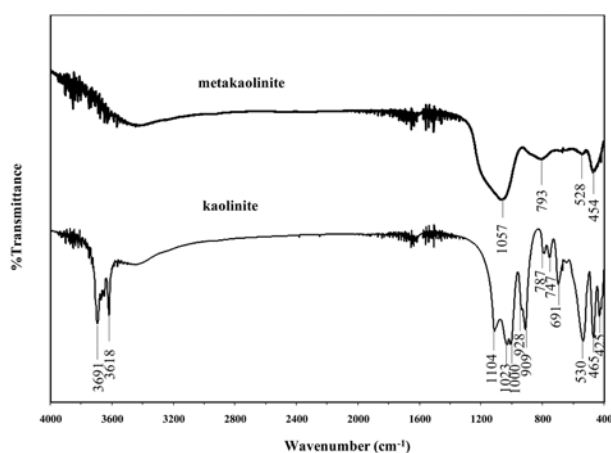


Fig. 2. FTIR spectra of kaolinite and metakaolinite.

700 °C for 5 h shows the main amorphous phase and remaining peaks due to quartz, illite, and slightly kaolinite phase. Metakaolinite is believed to be a defect phase in which the tetrahedral silica layers of the original clay structure are largely retained adjacent to AlO_4 tetrahedral units derived from the original octahedral layer of the kaolinite. Maximum reactivity for metakaolinite can be obtained by calcinations of the kaolinite at 700 °C to 750 °C, producing a maximum concentration of 4 and 5 coordinate aluminum and minimum concentration of 6 coordinate aluminum. Higher temperature treatment leads to mullite and cristobalite [20]. Fig. 2 illustrates the FTIR spectra over the range 400-4000 cm^{-1} , corresponding to the transformation of kaolinite to metakaolinite. The bands of kaolinite at 1104, 1023, 1000, 691, 465, and 425 cm^{-1} are attributed to Si-O stretching. The bands at 787, 747, and 530 cm^{-1} are assigned to Si-O-Al stretching. The

appearance of the band at 909 cm^{-1} is related to Al-OH stretching [21-23]. The bands at 3691 and 3618 cm^{-1} have been assigned to the stretching vibration of hydroxyl groups in the kaolinite structure which are not present in the metakaolinite spectra. The OH stretching bands were eliminated indicating the complete dehydroxylation process. The antisymmetric Si-O stretching bands merged to be a broad band and shifted to 1057. The coordination of Al changed from octahedral at 530 cm^{-1} to the lower one at 793 cm^{-1} . This was identified as the Al-O bond in the Al_2O_3 part of metakaolinite.

Synthesis of zeolite and characterization

Fig. 3 presents the intensity of unreacted and reacted metakaolinite treated with KOH and KCl solution. The most distinct of changes in the XRD patterns are the reduction in intensity of the metakaolinite peaks and the appearance of crystalline zeolite N. Fig. 3 displays

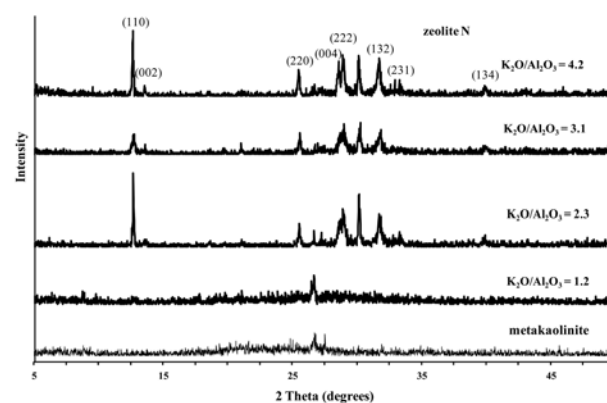


Fig. 3. Powder XRD patterns of metakaolinite and representation as-synthesized products obtained after their hydrothermal reaction in different K_2O/Al_2O_3 ratios.

Table 2. Reaction parameters.

Reaction	K_2O/Al_2O_3	KCl/Al_2O_3	H_2O/Al_2O_3	Temperature (°C)	Time (hours)	CEC (meq 100 g^{-1})	Primary product
1	2.3	1.7	48.0	175	2	300	zeolite N
2	2.3	2.1	48.0	175	2	458	zeolite N
3	2.3	3.5	48.0	175	2	576	zeolite N
4	2.3	4.2	48.0	175	2	532	zeolite N
5	1.2	3.5	48.0	175	2	320	metakaolinite
6	3.1	3.5	48.0	175	2	550	zeolite N
7	4.2	3.5	48.0	175	2	550	zeolite N
8	2.3	3.5	48.0	80	2	270	KAD
9	2.3	3.5	48.0	90	2	320	KAD
10	2.3	1.7	48.0	110	2	290	KAD
11	2.3	2.1	48.0	130	2	450	zeolite N
12	2.3	3.5	48.0	150	2	430	zeolite N
13	2.3	4.2	48.0	175	6	500	zeolite N
14	2.3	3.5	48.0	175	10	500	zeolite N
15	2.3	3.5	48.0	175	12	510	zeolite N
16	2.3	3.5	48.0	175	24	590	zeolite N

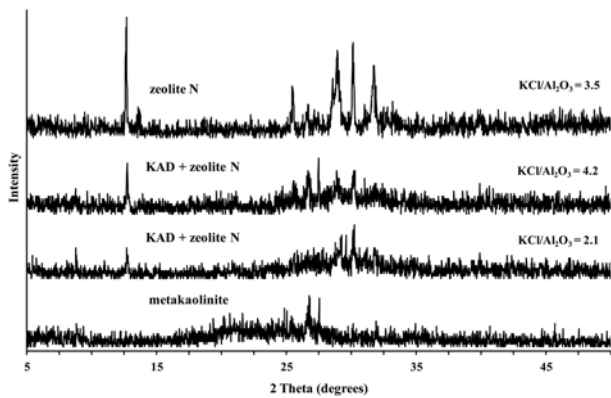


Fig. 4. Powder XRD patterns of metakaolinite and representation as-synthesized products obtained after their hydrothermal reaction in different $\text{KCl}/\text{Al}_2\text{O}_3$ ratios.

a series of XRD patterns for the starting composition of reaction 5, 3, 6, and 7 (Table 2) at various molar ratios of $\text{K}_2\text{O}/\text{Al}_2\text{O}_3$. At molar ratios of $\text{K}_2\text{O}/\text{Al}_2\text{O}_3 = 1.2$, the XRD pattern reveals that un-reacted metakaolinite. Zeolite N was not synthesized at a $\text{K}_2\text{O}/\text{Al}_2\text{O}_3$ ratio of 1.2, however; it was synthesized well at a ratio of 2.3. In general, the crystalline phase increases with increasing a molar ratio of $\text{K}_2\text{O}/\text{Al}_2\text{O}_3$ (increasing KOH concentration). This indicates that the dissolution of solid amorphous increases with the rise in the concentration of KOH solution, resulting in enhancing the formation of nuclei and intensifying the rate of crystallization. However, it could be concluded that a molar ratio of $\text{K}_2\text{O}/\text{Al}_2\text{O}_3$ more than 2.3 was more likely to be constant. There was no change in crystallinity over molar ratio of $\text{K}_2\text{O}/\text{Al}_2\text{O}_3$ over 2.3. At high KOH concentration, an intense dissolution of the starting metakaolinite was accompanied by the precipitation of zeolite phase. We have assumed that the most suitable ratio of $\text{K}_2\text{O}/\text{Al}_2\text{O}_3$ is 2.3, because it gives the high crystalline phase within these experimental conditions. Therefore, the molar ratio of $\text{K}_2\text{O}/\text{Al}_2\text{O}_3$ is 2.3 for the next experiment was selected. Fig. 4 illustrates a series of XRD patterns for the metakaolinite and the hydrothermal reaction with different $\text{KCl}/\text{Al}_2\text{O}_3$ ratios whereas $\text{K}_2\text{O}/\text{Al}_2\text{O}_3 = 2.3$, $\text{H}_2\text{O}/\text{Al}_2\text{O}_3 = 48.0$, $T = 175^\circ\text{C}$, and reaction time of 2 h were not changed. The parameters for reaction 2-4 are listed in Table 2 and displayed that for $\text{KCl}/\text{Al}_2\text{O}_3 = 3.5$ the primary product is zeolite N. The $\text{KCl}/\text{Al}_2\text{O}_3$ lower and higher molar ratio of 3.5 kaolinite amorphous derivative (KAD) phase is predominant. Fig. 4, in the ratio of $\text{KCl}/\text{Al}_2\text{O}_3$ value, zeolite N product tends to increase from 2.1 to 4.2. This suggests that the dissolution of amorphous metakaolinite increase with the rise in the ratio of $\text{KCl}/\text{Al}_2\text{O}_3$, resulting in enhancing the formation of nuclei and raising the crystallization. However, the intensity of crystallinity decreases at high ratio of $\text{KCl}/\text{Al}_2\text{O}_3$. This is because of the high excess concentration of the synthesis process

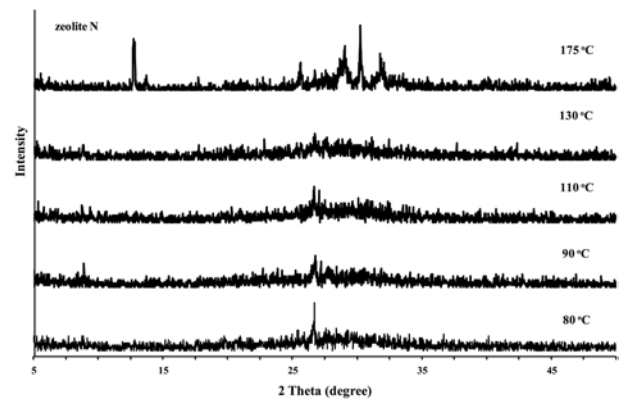


Fig. 5. Powder XRD patterns for 2 h hydrothermal synthesis with metakaolinite at different reaction temperatures using $\text{K}_2\text{O}/\text{Al}_2\text{O}_3 = 2.3$, $\text{KCl}/\text{Al}_2\text{O}_3 = 3.5$, and $\text{H}_2\text{O}/\text{Al}_2\text{O}_3 = 48.0$.

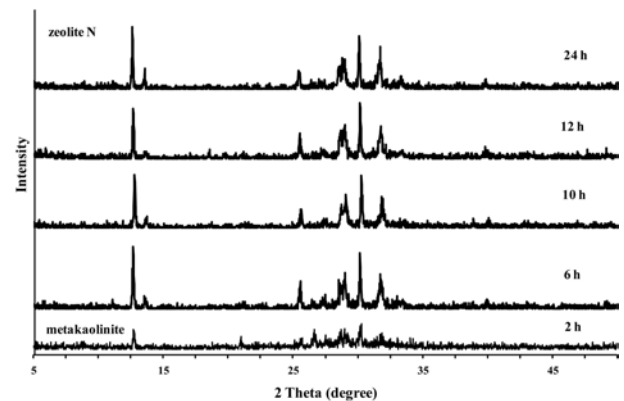


Fig. 6. Powder XRD patterns of samples from the reactor synthesis of zeolite N with different reaction times.

which proposes a lower range of stability. In the molar, the ratio of $\text{KCl}/\text{Al}_2\text{O}_3 = 3.5$ seems to be the most suitable condition as it provides the highest intensity of zeolite N crystallization. The main product is KAD phase at the temperature of 80°C to 130°C as the clear effect of temperature in Fig. 5 while only well crystallized zeolite N was observed at 175°C , which coincided with the highest cation exchange capacity (CEC) value (Table 2). This result indicated that the crystallinity zeolite N occurrence was accelerated with an increase of the reaction temperature. Consequently, the reaction temperature of 175°C was selected for the further experimental. Fig. 6 proves that XRD patterns of zeolite N samples could be obtained at different reaction periods. The peak intensities developed progressively as the crystallization period increased. The characteristic XRD peaks of the zeolite N began to appear after 2 h and fully crystallized after 12 h. No other crystalline phase (impurity phase) appeared in the XRD pattern of samples even after the prolonged crystallization period up to 24 h. However, it seemed to be constant with a longer reaction time.

SEM images (Fig. 7) exhibits interesting morphologies providing new evidence on the phase reaction history after the hydrothermal transformation of metakaolinite in

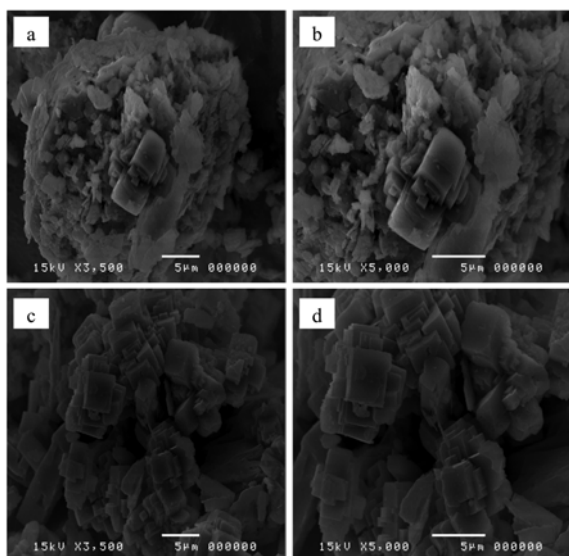


Fig. 7. SEM images showing the occurrence of representative synthesis products obtained via hydrothermal treatment (175 °C) of metakaolinite at 2 h (a-b) and 24 h (c-d) in the molar ratio of $K_2O/Al_2O_3 = 2.3$, $KCl/Al_2O_3 = 3.5$, $H_2O/Al_2O_3 = 48.0$.

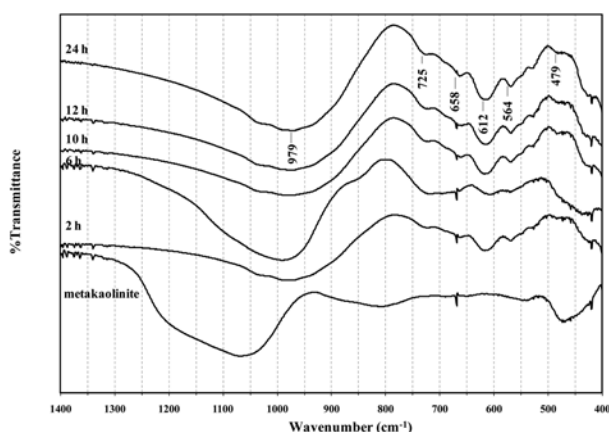


Fig. 8. FTIR spectra of metakaolinite and zeolite N obtained after its hydrothermal treatment at 2-24 h.

alkaline solution at reaction times of 2 h and 24 h. Fig. 7a-b illustrates an example of the dissolution of metakaolinite, revealed by its different morphology in the boundary region, which might indicate the formation of zeolite N. Fig. 7a-b illustrate an array of tetragonal prismatic crystals of zeolite N, which grew from the center of metakaolinite sphere. In Fig. 7c -d, zeolite N confirmed general form particle morphology and small sized particles, whose typical crystallite sizes ranged from 1-5 μm . Fig. 8 illustrates the FTIR spectra over the range 400-1400 cm^{-1} , corresponding to the transformation of metakaolinite to zeolite N. The characteristic bands observed in metakaolinite were 1057, 793, and 454 cm^{-1} , with broad band centered. A band at 1057 cm^{-1} in metakaolinite was observed and assigned to amorphous SiO_2 , as reported by some authors (Sinha et al. [24], Valcke et al. [25], Qiu et al. [26]). A peak at 793 cm^{-1} corresponding to the vibration

band of AlO_4 tetrahedron in metakaolinite; these peaks indicated the formation of the disordered metakaolinite phase. The spectrum of zeolite N exhibited absorptions at 479, 564, 612, 658, 725, and 979 cm^{-1} . They could be assigned to the vibrations of 4 = 1 zeolites group. A 4 = 1 complex caused the appearance of the whole series of bands in the range of pseudo lattice bands in the IR spectra located in the range of 500-760 cm^{-1} . The occurrence of the large number of bands should be associated with many types of 4-membered rings with different geometry. The bands appearing of lower wave numbers occurring at 480-500 cm^{-1} could be assigned to the vibration of 8-membered rings [27]. These FTIR results have been strongly confirmed by those obtained from the XRD data.

Conclusions

Zeolite N could be synthesized by hydrothermal method by using metakaolinite (thermally activated kaolinite), KOH, KCl, and H_2O as starting materials. The initial batch compositions using metakaolinite, KOH, KCl, and H_2O were mixed in the different molar ratio over a broad time-temperature range from 80 to 175 °C, and 2 to 24 h. The starting material K_2O/Al_2O_3 , KCl/Al_2O_3 , and H_2O/Al_2O_3 molar ratio of 2.3, 3.5, and 48.0 at 175 °C for 24 h could be successfully converted into zeolite N. FTIR spectra exhibited the presence of 4 = 1 vibrations, 4-membered rings and 8-membered rings vibration mode. The CEC of zeolite N was 590 meq 100 g^{-1} . In sum, Narathiwat kaolinite could be considered as an economical material and as a potential source industrial production of zeolite N in Thailand.

Acknowledgments

This study was supported by the Center of Excellence for Innovation in Chemistry (PERCH-CIC), Commission on Higher Education, Ministry of Education.

References

1. A.N. Christensen, and H. Fjellvag, Acta. Chem. Scand. 51 (1997) 969-973.
2. I.D.R. Mackinnon, K. Barr, E. Miller, S. Hunter, and T. Pinel, Water. Sci. Technol. 41 [11] (2003) 101-107.
3. R. J. Lussier, J. Catal. 129 (1991) 225-237.
4. M. Murat, A. Amokrane, J.P. Bastide, and L. Montanaro, Clay. Miner. 27 [1] (1992) 119-130.
5. D. Akolekar, A. Chaffee, and R.F. Howe, Zeolites. 19 [5] (1997) 359-365.
6. M. Perissinotto, L. Storaro, M. Lenarda, and R.J. Ganzerla, J. Mol. Catal. A-Chem. 121 [1] (1997) 1105-1109.
7. S. Chandrasekhar, and P.N. Pramada, J. Porous. Mater. 6 (1999) 283-296.
8. A. Demortier, N. Gobeltz, J.P. Lelieur, and C. Duhayon, Int. J. Inorg. Mater. 1 [1] (1999) 129-134.
9. M. Xu, M. Cheng, X. Bao, and X. Liu, D, J. Mater. Chem. 9 (1999) 2965-2966.

10. R. C. Mackenzie in "Differential Thermal Analysis" Vol 1, 1st Ed, (Academic Press London, 1970).
11. W. Kim, D. Choi, and S. Kim, *Mater. Trans.* 51 [9] (2010) 1694-1698.
12. M. Gougazeh, and J.-Ch. Buhl, *J. Assoc. Arab. Uni. for Basic & Appl. Sci.* 15 (2014) 35-42.
13. Kwakye-Awuah, E. Von-Kiti, R. Buamah, I. Nkrumah, and C. Williams, *Int. J. Sci & Eng Res.* 5 [2] (2014) 734-741.
14. A. A. Mostafa, H. F. Youssef, M. H. Sorour, S. R. Tewfik, and H. F. Shalaan, in *Proceedings of the 2th International Conference on Environmental Science and Technology* (Singapore, 2011) p. VI-43.
15. I.D.R. Mackinnon, G.J. Miller, and W. Stolz, *Appl. Clay. Sci.* 48 (2010) 622-630.
16. I.D.R. Mackinnon, G.J. Millar, and W. Stolz, *Appl. Clay. Sci.* 58 (2012) 1-7.
17. A. Molina, and C. Poole, *Miner. Eng.* 17 (2004) 167-173.
18. D.W. Breck, in "Zeolite molecular sieve structure, chemistry and user" (Wiley InterScience New York, 1974) 261-314.
19. S. Suhanda, S. Rifki, and R. Abdul, *J. Ceram. Process. Res.* 14 [3] (2013) 400-404.
20. J. Rocha, J.M. Adams, and J. Klinowski, *J. Solid. Stat. Chem.* 89 [2] (1990) 260-274.
21. C. Belver, M.A.B. Munoz, and M.A. Vicente, *Chem. Mater.* 14 [5] (2002) 2033-2043.
22. J. Madejova, in "FTIR techniques in clay mineral studies" (*Vib. Spectrosc.* 2003) 1-10.
23. B.N. Dudkin, I.V. Loukhina, E.G. Avvakumov, and V.P. Isupov, *Russ. J. Appl. Chem.* 78 [1] (2005) 33-37.
24. P.K. Sinha, P.K. Panicker, and R.V. Amalvaj, *Waste Manage.* 15 [2] (1995) 149-157.
25. E. Valcke, B. Engels, and A. Cremers, *Zeolites.* 18[2] (1997) 212-217.
26. G. Qiu, T. Jiang, G. Li, X. Fan, and Z. Huang, *Scand. J. Metall.* 33 [2] (2004) 121-128.
27. W. Mozgawa, M. Krol, and K. Barczyk, *Chemik.* 65 [7] (2011) 667-674.